



HAL
open science

Residual-based scheme for detection and characterization of faults in lithium-ion batteries

Heraldo Rozas, Ruben M. Claveria, Marcos E. Orchard, Kamal Medjaher

► **To cite this version:**

Heraldo Rozas, Ruben M. Claveria, Marcos E. Orchard, Kamal Medjaher. Residual-based scheme for detection and characterization of faults in lithium-ion batteries. IFAC SAFEPROCESS 2018, Aug 2018, Warsaw, Poland. pp.200-207. hal-02356314

HAL Id: hal-02356314

<https://hal.science/hal-02356314>

Submitted on 8 Nov 2019

HAL is a multi-disciplinary open access archive for the deposit and dissemination of scientific research documents, whether they are published or not. The documents may come from teaching and research institutions in France or abroad, or from public or private research centers.

L'archive ouverte pluridisciplinaire **HAL**, est destinée au dépôt et à la diffusion de documents scientifiques de niveau recherche, publiés ou non, émanant des établissements d'enseignement et de recherche français ou étrangers, des laboratoires publics ou privés.



Open Archive Toulouse Archive Ouverte (OATAO)

OATAO is an open access repository that collects the work of some Toulouse researchers and makes it freely available over the web where possible.

This is an author's version published in: <http://oatao.univ-toulouse.fr/22007>

Official URL: <https://doi.org/10.1016/j.ifacol.2018.09.578>

To cite this version:

Rozas, Heraldo and Claveria, Ruben M. and Orchard, Marcos E. and Medjaher, Kamal Residual-based scheme for detection and characterization of faults in lithium-ion batteries. (2018) In: IFAC SAFEPROCESS 2018, 31 August 2018 - 29 August 2018 (Warsaw, Poland).

Any correspondence concerning this service should be sent to the repository administrator:

tech-oatao@listes-diff.inp-toulouse.fr

Residual-based scheme for detection and characterization of faults in lithium-ion batteries

Heraldo Rozas* Ruben M. Claveria* Marcos E. Orchard*
Kamal Medjaher**

* *Universidad de Chile, Tupper 2007, Santiago, Chile*
(e-mail: heraldo.rozas@ing.uchile.cl, rclaveria@ing.uchile.cl,
morchard@ing.uchile.cl)

** *École Nationale d'Ingénieurs de Tarbes, (e-mail:
kamal.medjaher@enit.fr)*

Abstract: This work proposes a real-time scheme to monitor the occurrence of faults and perform fault characterization. Faults, in this context, correspond to changes in the parameters of the system being monitored. The method relies on the concept of Analytical Redundancy Relation (ARR), which can be defined as the evaluation of the mathematical constraints of the physical model of the system given the real, noisy measurements. The algorithm consists of two modules: a detection strategy that relies on the regular application of an ARR-based hypothesis test in discrete time-steps; and an optimization procedure to estimate the changes undergone after a fault. By selecting a set of feasible solutions from the output of the optimization algorithm, the method also sheds some light on the uncertainty associated to the estimated quantities. The methodology is tested on simulated data of lithium-ion batteries in unmanned aerial vehicles..

Keywords: Analytical redundancy relation, Bond graph, Fault detection and isolation, Lithium-ion batteries.

1. INTRODUCTION

Most physical systems undergo degradation due to their operational conditions. Certain industrial applications require an accurate characterization of the state of health (SOH), since the presence of degraded components may lead to the occurrence of catastrophic events or systematic errors in the system state estimation.

The framework referred to as Prognostics and Health Management (PHM) offers an alternative to deal with this problem Benkedjouh et al. (2015). PHM aims at performing real-time health evaluation of a system under its actual operating conditions, as well as the prediction of its future state based on up-to-date measurements. To do so, PHM integrates tools from a variety of disciplines, including sensing technologies, failure physics, machine learning, modern statistics, and reliability engineering (Kim et al. (2017)).

PHM can be broken down in a series of steps: data acquisition, diagnostics, prognostics, and health management. Data acquisition involves collecting measurements from the sensors and processing them to extract useful features for diagnosis. The diagnostics step corresponds to fault

detection and isolation (FDI), determining which component is failing and assessing how severe it is with respect to a failure threshold. Prognostics, on the other hand, estimates how much time is left for the occurrence of a failure under the current operating condition. Finally, health management step correspond to the task of managing in an optimal manner the maintenance scheduling and logistics support of the system (Kim et al. (2017)). The ultimate aim is providing an important source of information for taking decisions about the system's operation policy—that is, managing the operational conditions, regulating the workload, etc.

A major challenge related to the prognostics stage is to properly characterize the impact of uncertainty sources, for these sources have a direct impact on the precision of long-term predictions (Orchard et al. (2009); Daigle and Goebel (2013); Kim et al. (2017)). Thus, the final aim of our research is the characterization of the uncertainty in the diagnostics stage based on Bond Graph system model. In this paper, we present a first advance in this direction, proposing a diagnosis strategy based on bond graph (DBG) method (Samantaray et al. (2006)) to obtain an estimate of the state of a system, given the current set of measurements, after the occurrence of a fault involving a shift in the system parameters. This method relies on evaluating a residual at each time. That residual, referred to as analytical redundancy relation (ARR), represents a physical constraint and it is expected to be close to zero in a healthy state of the system; therefore any departure

* This work has been supported by FONDECYT Chile Grant Nr. 1170044, and the Advanced Center for Electrical and Electronic Engineering, AC3E, Basal Project FB0008, CONICYT. Also, the authors want to thank project CONICYT PIA ACT1405. The work of H.R was supported by CONICYT-PFCHA/Magister Nacional/2018-22180232.

from that behaviour may imply the presence of a fault. Additionally, we present set of feasible trajectories of the space-state model, which are useful for getting an idea of the uncertainty associated to the process.

The proposed method is applicable to systems where the health indicator can be described in terms of a space-state model and where changes in system's parameters can be considered as fault modes. This method monitors the health indicator of the system according to methodology described in Samantaray et al. (2006), using a nominal model with known parameters. Fault detection implies that a parametric change has recently occurred, and therefore recognizes that the actual health indicator estimate may be biased due to the use of wrong parameter values. The methodology consists of two stages: first, a fault is isolated by a heuristic method; then, the quantities associated to the fault that has been previously isolated (they can be either states or parameters) are estimated by optimizing the residual within an appropriate time window. Optimization is performed by means of Particle Swarm Optimization, whose output provides not only a point-like estimate of the quantities of interest, but also a set of plausible values. That set is used to obtain a measure of uncertainty and risk in the diagnosis stage, and propagated over time in the prognostics stage.

Motivated by their use in Unmanned Aerial Vehicles (UAV), this works has lithium-ion batteries as its study case. The algorithm is tested on synthetic data of a lithium-ion battery which undergoes sudden changes in its inner capacity and resistance. Results show successful detection and isolation, and illustrate possible trajectories of the health indicator after the occurrence of the fault.

2. DEGRADATION MODEL AND BOND GRAPH (BG) REPRESENTATION FOR FAULT DETECTION AND ISOLATION (FDI)

The degradation process of the system of interest is assumed to have a reliable state-space model which describes its evolution over time:

$$x_t = f(x_{t-1}, \theta_t, w_t, u_t), \quad (1)$$

where $f(\cdot)$ is the state transition function, Θ is the model's parameter vector (which can vary over time), a noise w_t and an input u_t . Since x_t may not be observable in a direct manner, it is usually studied through a measurement y_t :

$$y_t = g(x_t, v_t) \quad (2)$$

where $g(\cdot)$ is a function that relates measurements with the real state of the system and a noise component v_t . In a sense, it can be thought as a model of the sensor.

The system degrades over time depending on the stress or load in operation. This fact is modeled by a change in one or more components of the parameter vector Θ and is treated as a fault mode. Therefore, if any of the system's parameters changes, the algorithm has to detect and isolate its change; otherwise, the estimation of the SOH will accumulate error and have an increasing bias. That point motivates the adoption of the approach presented in Samantaray et al. (2006), where the authors propose a systematic way of deriving a FDI framework using bond graph (BG) representation. BG is a modeling method that allows for representing multiple energy domains (systems

with electrical, thermodynamic, mechanic components) in the form of a graph, and has been widely used in mechatronic systems (Karnopp et al. (2012)). The FDI method presented in Samantaray et al. (2006) is based on the analysis of analytical redundancy relation (ARR), which corresponds to the numerical evaluation of physical constraints (of either static or dynamic nature) of a system during the its operation. For convenience, those equations are usually expressed in such a way that they equal zero. Theoretically, such constraints (for example, the Kirchhoff's rules of electrical circuits, which establishes that potential differences must sum up zero) must be satisfied at all times; however, due to noisy measurements as well as errors in the estimation of the system's variables (states and parameters), the numerical evaluation of these equations leads to small but non-zero values. The signal obtained by the continuous evaluation of ARR is referred to as the "residual" (equation 3):

$$r(t) = F(\hat{x}(t), y(t), \theta(t)) \approx 0 \quad (3)$$

The equation above, which describes the general formula of the residual in a real setting, implies that the residual is a function of: the state of the system, $x(t)$, whose exact value is actually unknown, but approximated by an estimate $\hat{x}(t)$; the measurements collected by the sensors, $y(t)$; and the system parameters Θ . The idea of using ARR as tool for FDI is that, whenever the ARR signal is found to be divergent from their expected behaviour, it may be an indicator of a fault in the system. Formally, this means that the problem of determining whether the system is operating under normal conditions or in presence of a fault is formulated as a hypothesis test. A residual is said to be *sensitive* to a fault in a system component if the ARR depends on the parameters associated with that component.

It is important to highlight that there exist a lot of work related to BG for FDI purposes. For instance, Jha et al. (2016); Nawaz et al. (2017); Mojallal and Lotfifard (2017); Cauffriez et al. (2016). Nevertheless, Samantaray et al. (2006) is adopted due to its clear methodology, which is suitable for the development of our proposal.

3. METHODOLOGY

As mentioned before, the faults addressed in this work correspond to sudden changes in the system parameters due to a change in the operating profile. The motivation for the proposed methodology is the characterization of the uncertainty in the diagnosis stage. The algorithm consists of two stages: first, fault detection and isolation; second, characterization of the new possible values of the system parameters (an estimation stage) and simulation of a set of new possible trajectories in the space state. The following subsections explain each stage in detail.

3.1 Detection and isolation stage

For the implementation of the FDI stage, we need a statistical characterization of the residual of the system in a healthy state (see Section 4.2 for an example). Because of the noisy nature of measurements, as well as the

presence of derivative components in the degradation model, a moving average of the residual (with moving windows whose width is empirically fitted depending on the problem) is preferred over the raw residual value. This filtered stochastic signal presents a more stable behaviour; thus, departures from the regular regime are likely to be indicators of systemic changes rather than a mere statistical possibility. To calculate the filtered residual at time t we consider a collection of residuals of length k , $\{r_{t-k}, \dots, r_t\}$ (referred to as the “window” hereinafter), and calculate $\bar{r}_t = \sum_{i=t-k}^t \alpha_i r_i$, where α_i are weights such that $\sum_{i=t-k}^t \alpha_i = 1$.

For fault detection purposes, we use a method inspired in Ozdemir et al. (2011), which makes use of Up-Down Counters. The method relies on evaluating an hypothesis test on each time step, announcing the detection of a fault whenever the null-hypothesis is rejected. Concretely, in this approach we keep a counter of the occurrences of the event of \bar{r}_t trespassing a threshold in a time window of size k . That threshold is defined previously, based on the characterization of the system in a “healthy” state, and typically involves a confidence interval for the value of \bar{r} . Additionally, a maximum value for the counter itself must be defined, such that when the filtered residual has trespassed its threshold an anomalous number of times, the algorithm announces the detection of a fault. The underlying idea is that, under normal conditions (the so-called healthy state), the residual is expected to fall within a certain range with high probability (say, 0.95), just with occasional deviations. Since the healthy state defines a prior probability, if such deviations start to occur more frequently, then a low probability event is taking place, indicating the violation of the null-hypothesis (“the system is working under normal conditions”).

We suppose that the fault can not be instantly detected due to system dynamics or measurement noise. Therefore, two important time instants are hereby identified: time of fault (TOF) and time of detection (TOD). In between, there is a period where the model of health indicator evolves considering incorrect parameter estimates, leading to an increment in the uncertainty associated to the actual health indicator. Considering the above, we define a third moment of interest called “time of correction” $TOC \in (TOF, TOD)$. TOC is chosen such that it is the minimum time the fault mode requires to be detected (empirically obtained) minus a security margin, with the aim of guaranteeing that the system is in fault-state at time TOC , which implies that the current state and parameter estimation and the are wrong. After the fault has been characterized, an optimization problem is solved and simulations of the trajectory of the state are performed for each feasible solution found. To illustrate, the three key time instants of the proposed method are shown in Figure 1. Note that at time TOC the system is in a fault-state (nominal model is far from ground-truth), therefore at this time there exists uncertainty about the current estimated state and the parameters of the model, motivating the following step of the method.

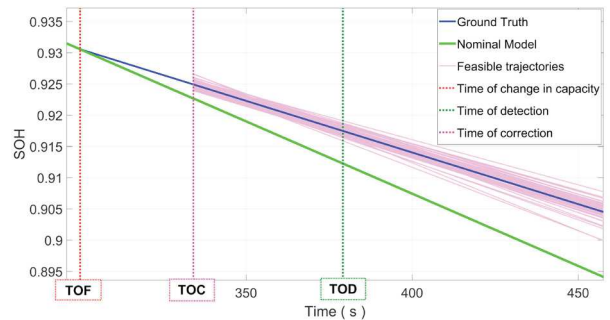


Fig. 1. Example of the three key time instants of the proposed-method.

3.2 State and parameter estimation by simulation of possible trajectories in the space-state

Once a fault has been detected, we assume that TOC exists, where x_{TOC} (the state of system) and Θ are wrong. We estimate the actual value of these quantities by minimizing the residual in a time window that starts in TOC and finishes in TOD . The underlying idea is that if we have a good initial condition of the system at time TOC and a good estimation of the system parameters after the fault, then the residual must remain around zero (similar to the behaviour during the healthy state); therefore we minimize it respect to initial condition x_{TOC} (state of the system at time TOC) and the parameter that triggered the fault, θ .

The formalization of the minimization problem is presented as follows:

$$\begin{aligned} & \underset{\theta, x_{TOC}}{\text{minimize}} && J(\theta, x_{TOC}) = \frac{1}{k} \sum_{j=1}^n r_{t-j}(\theta, x_{TOC})^2 \\ & \text{subject to} && \theta_i \in [\theta_i^l, \theta_i^u], \quad i = 1, \dots, m. \\ & && x_{TOC} \in [x_{TOC}^l, x_{TOC}^u] \end{aligned} \quad (4)$$

Figure 2 displays the key time instants of this scheme in chronological order.

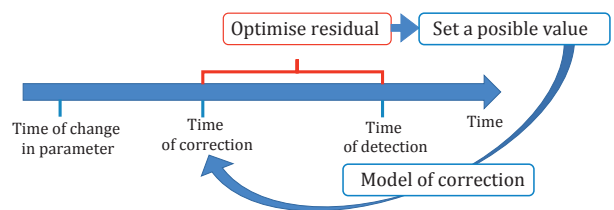


Fig. 2. Key time instants of the estimation stage.

For optimization purposes we use Particle Swarm Optimization (PSO) Kennedy and Eberhart (1995). In order to have a notion not only about the optimal (or possibly suboptimal) value of Θ and x_{TOC} , but also about the set of feasible solutions, we save all the particles of each generation. Once the optimization procedure is finished, we sample a certain amount of particles with probabilities proportional to the fitness function, and consider this set as a region of feasible values. Note that, although encompassing a significant number of samples, the optimization

procedure is performed in a single time instant (the time of detection) (see Figure 1). After the correction is accomplished, estimates of the state are re-calculated from the instant labelled *TOC* onwards, according to the set of feasible values previously identified.

We can employ both the mean and the fittest particle of the PSO run as estimates of the actual state and parameter values after the occurrence of the fault. Additionally, the set of PSO particles is used to calculate other feasible trajectories of the space-state model, which is useful to get an idea of the uncertainty associated to the process (see Figure 1)

4. CASE STUDY: FAULTS THAT COULD AFFECT THE OPERATIONAL RISK OF UAVS.

We will focus on the study of faults that might affect the operational risk of UAVs (Unmanned Aerial Vehicles) that are energized by Lithium-Ion batteries. This case of study will be developed through simulations using Matlab. In this case the variable that describes the SOH of the system is the state of charge (SOC), which corresponds to the amount of energy available to deliver. Typically, *SOC* is expressed by a number between 0 and 1, where 1 indicates fully charged and 0 fully discharged.

To characterize the battery's internal dynamics we use the electrical equivalent model shown in Figure 3, where $V_{oc}(SOC)$ (open circuit voltage) is a function of the *SOC*, and it is assumed that the internal impedance can be modelled as a resistance R_2 (that includes the polarization resistance) in series with a RC filter (parameters R_1 and C_1). The load is modelled by a current requirement, $I_L(t)$, which is supposed to change as a function of time.

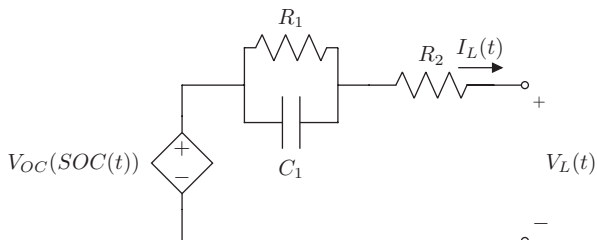


Fig. 3. Electrical model.

The discrete-time space-state model for the SOC is given by the following equation:

$$SOC_k = SOC_{k-1} - \frac{\Delta T \cdot I_{k-1}}{E_c \cdot 3600} \quad (5)$$

where ΔT is the sampling time (s), E_c is the energy storage capacity of the battery (Ah) and $I_k(A)$ is the load current. The relation between $V_{oc}(SOC)$ and SOC is shown in the following equation:

$$V_{oc}(SOC_k) = \nu_L + (\nu_0 - \nu_L) \cdot e^{\gamma \cdot (SOC_k - 1)} + \alpha \cdot \nu_L \cdot (SOC_k - 1) + (1 - \alpha) \cdot \nu_L \cdot (e^{-\beta} - e^{-\beta \cdot \sqrt{SOC_k}}), \quad (6)$$

where ν_L , ν_0 , α , β and γ are model parameters to be estimated offline according to the procedure described in Pola et al. (2015). For this simulation, the values of these model parameters are assumed to be known and

invariable in time. Faults in the system are associated to parameters R_2 and E_c , which can undergo degradation as a consequence of the underlying physics of a lithium-ion battery, as explained as follows:

- **Change in the internal resistance due to current load:** The value of R_2 is tightly related to the value of current I_L at the present time instant. A characterization of this phenomenon is presented in Burgos-Mellado et al. (2016), where the polarization resistance in a discharge process is calculated using experimental data obtained by discharging the battery bank with currents regulated at constant values. The results obtained show that the internal resistance increases when current load is lower and vice versa. Additionally, R_2 is shown to have a degree of dependence on SOC. In this simulation, the finer details of these phenomena will not be considered. As a first approximation, we assume a simplified model where R_2 varies as a function of I_L in the following way: sudden discrete increments in the value of parameter R_2 are enforced whenever the load current adopts values below the nominal range (transient behaviour is not modelled).
- **Changes in storage capacity:** Changes in environmental conditions, such as temperature or pressure, may affect the maximum amount of energy that the battery can deliver to the electric load. Consequently, voltage drops earlier than expected and the autonomy of the system is reduced (reduction of the End-of-Discharge time). For instance, Shabani and Biju (2015) reviews a number of examples of this phenomenon in contexts of controlled temperature. For simulation purposes, we consider that the energy storage capacity (E_c) of the battery experiments sudden shifts due to sudden changes in operating temperature. Finer modelization of this phenomena and its incorporation into a prognostics scheme is part of a future line of research.

To develop the simulation we consider the parameters of the Table 1, where parameters of $V_{oc}(SOC)$ model and E_c were extracted from a data set presented in Pola et al. (2015). The rest of the parameters were assigned in accordance to typical values.

Table 1. Parameters of simulation

Parameter	Value	Unit
dt	0.1	s
R_1	0.04	Ω
R_2	0.08	Ω
C_1	4	F
E_c	2.4	Ah
ν_L	3.997	V
ν_0	4.14	V
α	0.15	
β	17	
γ	10.5	

Previous works on parameter estimation of ion-lithium battery models have used different techniques: Recursive Least Squares (RLS) Tong et al. (2015); Allafi et al. (2017), Adaptive Unscented Kalman Filtering Partovibakhsh and Liu (2015), Particle Filter Pola et al. (2015). In this article, ion-lithium battery models are used as a mere study case.

4.1 ARR derivation and residual variation due to a parametric fault.

The development of a diagnostic fault model requires to sense certain variables. In this case, the sensed values (or measurements) correspond to current and voltage load, $I_L(t)$ and $V_L(t)$ respectively (see Figure 3). We model the system using the BG formalism, considering the derivative causality according to the procedure described in Samantaray et al. (2006). The corresponding Bond graph representation of the system is given by Figure 4.

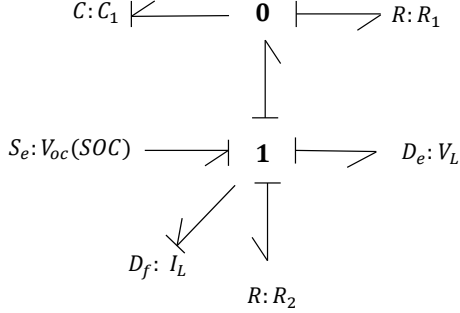


Fig. 4. BG derivative causality of the electrical system.

Applying the constitutive relation of junctions and the relation between effort (voltage) and flow (current) for each element, the following ARR can be derived:

$$\mathbf{ARR}_1 : V_{oc}(SOC) - R_1 I_L - V_L - R_2 I_L + R_1 C_1 \frac{d}{dt} [V_{oc}(SOC) - R_2 I_L - V_L] = 0. \quad (7)$$

Thus, the final form of the residual can be expressed as shown in equation 8.

$$r_1 = V_{oc}(SOC) - R_1 I_L - V_L - R_2 I_L + R_1 C_1 \frac{d}{dt} [V_{oc}(SOC) - R_2 I_L - V_L] \quad (8)$$

In this case study, the residual is sensitive to changes in R_2 , since it appears explicitly in Equation 8, therefore its correction is simple. On the other hand, the residual is not directly sensitive to shifts in capacity, as its relation with E_c is mediated by $V_{oc}(SOC)$, whose argument (SOC) is a function of E_c . In this particular problem, this fact translates into more gradual variations in r_1 when E_c changes than when R_2 changes.

4.2 Characterization of the probability distribution function (PDF) of the residual and the filtered residual in healthy state and detection model

Prior to the application of the method described in Section 3, a statistical characterization of the residual is obtained by simulating the system in a healthy state, with the parameters described in Table 1 and fitting PDFs for both the raw residual r and the filtered residual \hat{r} . The simulated data of the filtered residual is shown in Figure 5, note that a Gaussian distribution is fitted obtaining $\mu_f = -0.003$ and $\sigma_f = 0.0014$. In the case of the raw residual, the empirical distribution shows a similar shape with near-zero average, but the variance is higher: $\sigma_r = 0.014$ (this is consistent with idea of filtering noise).

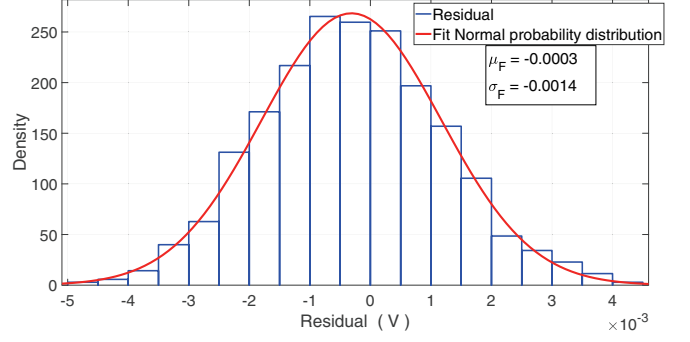


Fig. 5. Characterization of the PDF of the filtered residual in a healthy state

Considering the data associated to both healthy and faulty states of the system, we define the following thresholds for the detection and isolation stage:

- **Fault E_c :** We consider a $counter_1$ that increments when the filtered residual is out of the range of $2\sigma_f$, in a temporal neighbourhood not lower than 10 samples, otherwise the counter is reset. When the $counter_1 > 300$ a fault is detected and isolated.
- **Fault R_2 :** It is possible to detect and isolate directly due to its explicit appearance in the equation of the residual. However, we use a window of 20 samples, with the objective estimate the value of R_2 after the sudden shift.

The directions for defining thresholds and other algorithm-related parameters for the counters are described in Subsection 3.1. In this case study we designed the counters by trial and error. TOC is fixed such that, whenever the fault is detected, the retrospective time-window is well defined in the sense that its initial time (TOC) always falls in a time instant where both the system state and parameters are wrongly estimated. Note that the width of the window time is fixed: for fault E_c , TOC is equal to the current time minus 45[s]; whereas for fault R_2 is equal to the current time minus 1.5[s].

5. RESULTS AND DISCUSSION

To test the proposed methodology, we ran a simulation of the system described in the previous section, considering 3 scenarios:

- (1) At $Time = 99[s]$, parameter R_2 suddenly changes from its nominal value to $0.064(\Omega)$ as a consequence of a variation of the load current.
- (2) At $Time = 249[s]$, the parameter E_c suddenly drops from its nominal value to $1.68(Ah)$ as a consequence of a variation of the temperature of operation.
- (3) At $Time = 300[s]$, the parameter E_c suddenly raises from its nominal value to $3.12(Ah)$ as a consequence of a variation of the temperature of operation.

Figure 6 illustrates how the residuals (both raw and filtered signals) behaves in the first scenario. It is noticeable, from this figure, that quantity \hat{r}_t undergoes an almost immediate departure from the region defined by the upper and lower confidence thresholds ($\pm 2\sigma_F$). This is easily explained by the straightforward dependency of the residual

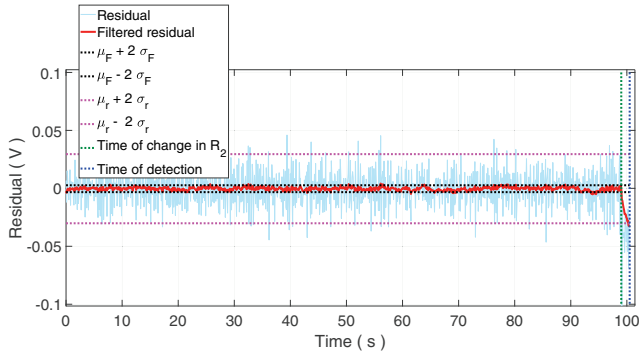


Fig. 6. Detection: Change in R_2 .

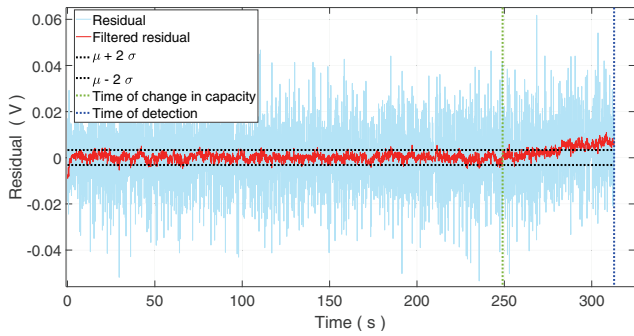


Fig. 7. Detection: Change in E_c .

on quantity R_2 , which appears multiplying current load I_L in the third term of the sum of Equation 8. Thus, calculating the residual using the measurements of I_L , V_L and an incorrect value of R_2 leads to an appreciable departure from the close-to-zero region of confidence, leading to a fast detection of the fault event. The above implies that the fault is easy to detect and isolate. In the estimation stage a value of $R_2^{new} = 0.0636$ is obtained. This outcome shows that the proposed method works to detect faults in R_2 .

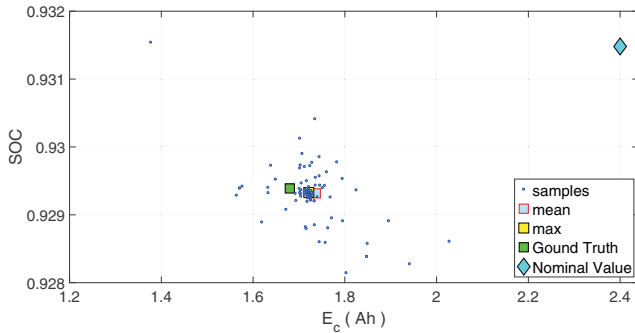
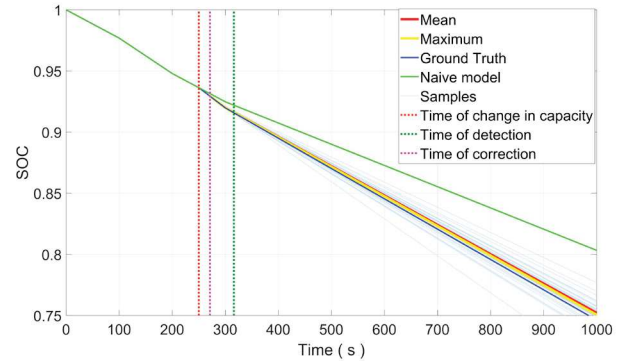


Fig. 8. Selection of particles from PSO

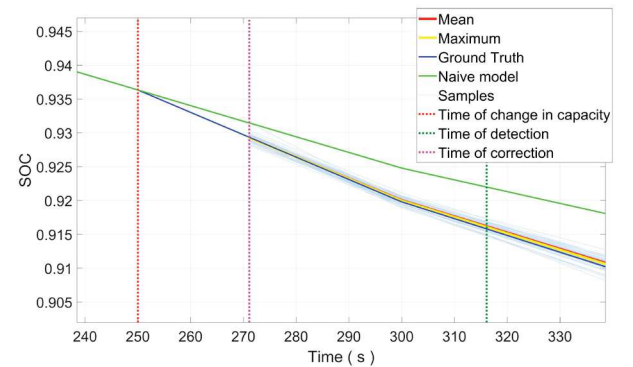
Figure 7, on the other hand, shows the behaviour of the residual in the second scenario. This time, the fault is generated by a shift in storage capacity, which, unlike term R_2 , is not part of a dominant term of the sum. In Equation 8, the term involving a derivative has marginal influence on the total sum, where the main indicator of an anomaly in E_c is $V_{oc}(SOC)$. Because of the “integrative” nature of SOC (see Equation 5), a single instant error in

the calculation of the $\frac{\Delta T \cdot I_{k-1}}{E_c \cdot 3600}$ makes little difference in the estimation of SOC . It requires the accumulation of several successive errors in $\frac{\Delta T \cdot I_{k-1}}{E_c \cdot 3600}$ to make appreciable a systematic difference with the estimated open-circuit voltage $V_{oc}(SOC)$. As a consequence, the amount of time needed to detect this class of fault is around 70 [s], as can be seen in Figures 7 and 9b.

When the fault is detected in the second and third scenarios we apply the procedure described in Subsection 3.2. The Figure 8 shows a selection of 100 values sampled from the population of a PSO run. This set of solutions is part of a heuristic approach to characterize the uncertainty of SOC (at the instant TOC) and the value E_c after the fault. Note that, since the minimization of the residual requires the value of SOC at each time of the TOC , the optimization procedure does not only search for values of E_c , but also for initial conditions for the state of charge (SOC_{TOC}). Each feasible solution for (SOC_{TOC}, E_c) is propagated over time, as shown in Figure 9, where the best particle and the average solution (the mean of the selected particles) are illustrated in distinctive colors. As time progresses, most solutions depart from the ground-truth SOC value, while just a few solutions (including the best particle and the average solution) remain close. Figures 9 and 10 show the outputs of optimization stage of the second and third scenarios, respectively.



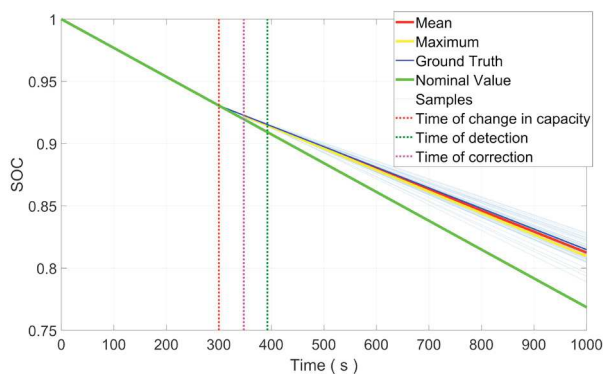
(a) Evolution of the SOC



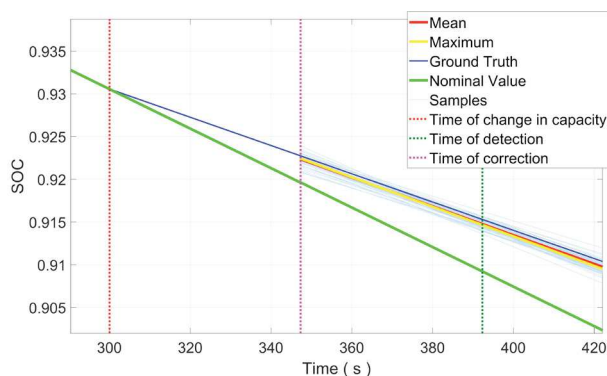
(b) Zoom

Fig. 9. Second Scenario: Generation of feasible trajectories in the space-state, based on selection of particles from PSO.

The scenario where parameter values remain uncorrected after the occurrence of the faults is labelled as “naive model”, and consistently fails to give a close estimation of *SOC*. In UAVs, such gap between the real and the estimated *SOC* may lead to a catastrophic events. For example, if *SOC* is overestimated (as in the second scenario, Figure 9, where the naive model is above the ground truth value), the real remaining useful life of the vehicle is shorter than that derived from the estimation, leading to an unexpected energy shortage. On the contrary, when *SOC* is underestimated (as in the third scenario, Figure 10), the estimation errors may lead to abort an UAV mission, even though the *SOC* is enough to complete it.



(a) Evolution of the SOC



(b) Zoom

Fig. 10. Third Scenario: Generation of feasible trajectories in the space-state, based on selection of particles from PSO.

Both the best particle and the “averaged solution” provide a close approximation of the *SOC* value. However, there is no theoretical guarantee for the accuracy of those solutions—the output of the optimization algorithm may be optimal in terms of the data used to calculate the new parameter values (the “correction window”), but even small differences with the real values may lead to biased estimations. For that reason, certain particles falling in the so-called feasible region—which are close to, but are not exactly the optimal solution—may perform, over time, better than the best particle and the “average solution” in terms of estimation of *SOC*. This remark encourages, for future works, a more active approach regarding the propagation of the feasible scenarios: each solution should be regularly evaluated and upgraded –if

necessary–, in order to identify the best solution as well as characterizing the uncertainty making into account the new measurements available.

6. FINAL REMARKS

The proposed method provides an estimate of the current state of a system, given the current set of measurements, after the occurrence of a fault involving a shift in the system parameters. Additionally, we present set of feasible trajectories of the space-state model, which sheds some light on the uncertainty associated to the process. The scheme successfully manages to identify possible solutions for the new parameters of the system, providing not only point-like estimates but also a wider set of feasible values. For E_c , those feasible scenarios are propagated over time, showing that the two estimates proposed (best fit and mean value from the PSO run), as well as a few particles in the set, follow the real *SOC* value closely. Most particles, however, depart from the real value as time progresses, being highly unlikely candidates for a solution. Future work is aimed at devising upgrade and resampling steps in the propagation of the feasible scenarios, evaluating each particle in the light of the new incoming measurements.

Additionally, this method provides a real-time scheme to detect faults for systems that feature some degree of integral dynamics in its operation. Since that kind of fault tends to be difficult to detect, that goal is accomplished by a heuristic approach that relies on a counter of unlikely events given a prior characterization of the system’s behaviour.

REFERENCES

- Allafi, W., Uddin, K., Zhang, C., Sha, R.M.R.A., and Marco, J. (2017). On-line scheme for parameter estimation of nonlinear lithium ion battery equivalent circuit models using the simplified refined instrumental variable method for a modified wiener continuous-time model. *Applied Energy*, 204, 497 – 508.
- Benkedjouh, T., Medjaher, K., Zerhouni, N., and Rechak, S. (2015). Health assessment and life prediction of cutting tools based on support vector regression. *Journal of Intelligent Manufacturing*, 26(2), 213–223.
- Burgos-Mellado, C., Orchard, M.E., Kazerani, M., Crdenas, R., and Sez, D. (2016). Particle-filtering-based estimation of maximum available power state in lithium-ion batteries. *Applied Energy*, 161(Supplement C), 349 – 363.
- Cauffriez, L., Grondel, S., Loslever, P., and Aubrun, C. (2016). Bond graph modeling for fault detection and isolation of a train door mechatronic system. *Control Engineering Practice*, 49, 212 – 224.
- Daigle, M.J. and Goebel, K. (2013). Model-based prognostics with concurrent damage progression processes. *IEEE Transactions on Systems, man, and cybernetics: systems*, 43(3), 535–546.
- Jha, M.S., Dauphin-Tanguy, G., and Ould-Bouamama, B. (2016). Particle filter based hybrid prognostics for health monitoring of uncertain systems in bond graph framework. *Mechanical Systems and Signal Processing*, 75, 301 – 329.

- Karnopp, D.C., Margolis, D.L., and Rosenberg, R.C. (2012). *System dynamics: modeling, simulation, and control of mechatronic systems*. John Wiley & Sons.
- Kennedy, J. and Eberhart, R. (1995). Particle swarm optimization. In *Proceedings of IEEE International Conference on Neural Networks IV, pages*, volume 1000.
- Kim, N.H., An, D., and Choi, J.H. (2017). *Prognostics and Health Management of Engineering Systems: An Introduction*. Springer International Publishing, 1 edition.
- Mojallal, A. and Lotfifard, S. (2017). Multi-physics graphical model based fault detection and isolation in wind turbines. *IEEE Transactions on Smart Grid*, 1–1.
- Nawaz, M.H., Yu, L., Liu, H., and Rehman, W.U. (2017). Analytical method for fault detection isolation in electro-hydrostatic actuator using bond graph modeling. In *2017 14th International Bhurban Conference on Applied Sciences and Technology (IBCAST)*, 312–317.
- Orchard, M., Tobar, F., and Vachtsevanos, G. (2009). Outer feedback correction loops in particle filtering-based prognostic algorithms: Statistical performance comparison. *Studies in Informatics and Control*, 18(4), 295–304.
- Ozdemir, A.A., Seiler, P., and Balas, G.J. (2011). Wind turbine fault detection using counter-based residual thresholding. *IFAC Proceedings Volumes*, 44(1), 8289–8294.
- Partovibakhsh, M. and Liu, G. (2015). An adaptive unscented kalman filtering approach for online estimation of model parameters and state-of-charge of lithium-ion batteries for autonomous mobile robots. *IEEE Transactions on Control Systems Technology*, 23(1), 357–363.
- Pola, D.A., Navarrete, H.F., Orchard, M.E., Rabi, R.S., Cerda, M.A., Olivares, B.E., Silva, J.F., Espinoza, P.A., and Perez, A. (2015). Particle-filtering-based discharge time prognosis for lithium-ion batteries with a statistical characterization of use profiles. *IEEE Transactions on Reliability*, 64(2), 710–720. doi: 10.1109/TR.2014.2385069.
- Samantaray, A., Medjaher, K., Bouamama, B.O., Staroswiecki, M., and Dauphin-Tanguy, G. (2006). Diagnostic bond graphs for online fault detection and isolation. *Simulation Modelling Practice and Theory*, 14(3), 237 – 262.
- Shabani, B. and Biju, M. (2015). Theoretical modelling methods for thermal management of batteries. *Energies*, 8(9), 10153–10177. doi:10.3390/en80910153.
- Tong, S., Klein, M.P., and Park, J.W. (2015). Online optimization of battery open circuit voltage for improved state-of-charge and state-of-health estimation. *Journal of Power Sources*, 293, 416 – 428.